Energy- and Spectral-Efficient Resource Allocation Algorithm for Heterogeneous Networks

Cemil Can Coskun, *Member, IEEE*, and Ender Ayanoglu, *Fellow, IEEE*

***Abstract*—In this paper, the tradeoff between energy efficiency and spectral efficiency in multicell heterogeneous networks is investigated. Our objective is to maximize both energy efficiency and spectral efficiency of the network, while satisfying the minimum rate requirements of the users. We define our objective function as the weighted summation of energy efficiency and spectral efficiency functions. The fractional frequency reuse (FFR) scheme is employed to suppress intercell interference. We formulate the problem as cell-center boundary selection for FFR, frequency assignment to users, and power allocation. The optimal solution of this problem requires exhaustive search over all cell-center radii, frequency assignments, and power levels. We propose a three-stage algorithm and apply it consecutively until convergence. First, we select the cell-center radius for the FFR method. Second, we assign the frequency resources to users to satisfy their rate requirements and also maximize the objective function. Third, we solve the power allocation subproblem by using the Levenberg–Marquardt method. Minimum rate requirements of users are also included in the solution by using dual decomposition techniques. Our numerical results show a Pareto-optimal solution for energy efficiency and spectral efficiency. We present energy efficiency, spectral efficiency, outage probability, and average transmit power results for different minimum rate constraints. Among other results, we show that, in a particular setting, 13% energy efficiency increase can be obtained in a multicell heterogeneous wireless network by sacrificing 7% spectral efficiency.**

***Index Terms*—Energy efficiency, heterogeneous cellular networks, multi-objective optimization, spectral efficiency.**

I. Introduction

IN RECENT years, the rapid increase of mobile devices such as smart phones, tablets, and wearable computers and mobile applications brought the need for higher throughput and the problem of coverage simultaneously. The capacity of the wireless networks needs to increase to meet this demand. In [1], expanding spectrum and increasing spectral efficiency are proposed among several solutions for this problem. Although increasing spectral efficiency eliminates these problems, the spectral efficiency metric does not provide any intuition about the efficiency of energy consumption. In fact, solutions that improve spectral efficiency may be inefficient in terms of energy efficiency. The increased energy consumption in wireless networks contributes to the growth of greenhouse gases. The information and communication technologies cause about 2–4% of all carbon footprint generation [2]. This topic has been investigated in the literature under the theme of "Green Communications," see, e.g., [2] and the references therein. In this paper, we investigate the tradeoff between energy efficiency and spectral efficiency in multi-cell heterogeneous wireless networks.

To meet the increasing throughput demand and eliminate coverage holes, heterogeneous networks (HetNets) are investigated in the literature [3]. In [4], it is shown that both energy efficiency and spectral efficiency can be improved with dense small cell deployment. Due to the fact that low-powered base stations are deployed into the coverage area of a macrocell base station (MBS), the coverage regions of MBS and small cells overlap. Therefore, interference becomes a significant problem in HetNets. To overcome this problem, intercell interference cancellation and mitigation techniques are investigated in the literature [5], [6]. In this paper, we employ the fractional frequency reuse (FFR) scheme for multi-tier networks, studied in [7], [8]. FFR is preferred over other intercell interference solutions due to its low complexity. In this scheme, a virtual cell-center radius is selected to divide the sector area into two regions and then subbands are assigned to the base stations depending on their regions. In [7], same cell-center radius is used in each sector independent of the user distribution. Our prior work in [8] has employed the same FFR scheme, but the cell-center radii were selected depending on the user distribution. In this paper, we employ the same FFR scheme, however we update cell-center boundaries dynamically depending on the requirements of users. A similar approach is also used in our prior work in [9]. This approach helps us satisfy the rate requirements of users and improve our objective. Although the FFR scheme mitigates some portion of the interference in the network, intercell interference is still a significant problem. To further suppress the interference, the pricing mechanism has been studied to maximize the system utility in the literature, see, i.e., [10]–[13]. In [10], the transmission power times a predefined constant is used for the penalty function. This method prevents base stations from transmitting at high power levels. On the other hand, in [11]–[13], an

Manuscript received March 14, 2017; accepted August 2, 2017. Date of publication August 23, 2017; date of current version January 15, 2018. This work was partially supported by the National Science Foundation under Grant 1307551. Any opinions, findings, and conclusions or recommendations expressed in this material are those of the authors and do not necessarily reflect the view of the National Science Foundation. The review of this paper was coordinated by Dr. Y. Song. *(Corresponding author: Cemil Can Coskun.)*

C. C. Coskun was with the Center for Pervasive Communications and Computing, Department of Electrical Engineering and Computer Science, University of California, Irvine, CA 92697 USA. He is now with Qualcomm Atheros Inc., San Jose, CA 95110 USA (e-mail: ccoskun@uci.edu).

E. Ayanoglu is with the Center for Pervasive Communications and Computing, Department of Electrical Engineering and Computer Science, University of California, Irvine, CA 92697 USA (e-mail: ayanoglu@uci.edu).

Color versions of one or more of the figures in this paper are available online at http://ieeexplore.ieee.org.

Digital Object Identifier 10.1109/TVT.2017.2743684

interference-based penalty function is suggested. This approach lets the base stations transmit at high levels if the utility decrease due to interference is less than the improvement of the system utility with transmission power increase. In this paper, we employ a similar method where each base station is penalized with respect to the amount of interference it creates. This approach prevents the base station from increasing its transmission power to levels that hurt the utility of the other sectors which in turn causes a decrease of the total utility of the network.

As stated earlier, optimizing energy efficiency and spectral efficiency usually contradict with each other [14]. Therefore, this tradeoff has attracted attention in the literature recently. In [14], authors show that the energy efficiency function is strictly quasi-concave over spectral efficiency. In addition, it is shown that the power consumption minimization problem and the maximization of the energy efficiency problem do not have to coincide. Therefore, these problems should be investigated separately. In [15], the energy efficiency and spectral efficiency tradeoff is investigated for OFDMA networks with optimal joint resource allocation of transmission power and bandwidth. The authors show that when the cell size decreases, the energy efficiency of the network increases. Papers [14], [15] study the energy efficiency and spectral efficiency tradeoff for single-tier networks. When low-powered base stations are deployed with MBSs, intra-cell interference becomes a significant problem. The proposed algorithm in our paper and [16] investigate energy efficiency and spectral efficiency tradeoff for heterogeneous networks. In [16], the energy efficiency and spectral efficiency tradeoff has been investigated in interference-limited networks. The authors show that the problem is non-convex and NP-hard to solve. Therefore, they propose an iterative power allocation algorithm which guarantees convergence to a local optimum. They define the problem as maximizing energy efficiency of the network under minimum rate constraints. The proposed algorithm in our paper investigates maximizing the energy efficiency and spectral efficiency simultaneously.

The aforementioned papers investigate energy efficiency and spectral efficiency functions separately. Another approach to investigate this problem is to combine these metrics under one metric. For this purpose, multi-objective optimization techniques have been widely investigated in the literature [17]. These techniques are successfully used to investigate the energy efficiency and spectral efficiency tradeoff. The first approach to combine energy efficiency and spectral efficiency is the Cobb-Douglas production method [18], [19]. In the Cobb-Douglas method, different powers of the energy efficiency and spectral efficiency metrics are multiplied. In [18], it is shown that the metric that is obtained by using the Cobb-Douglas production method is quasi-concave over the power function. By using the same metric, authors in [19] investigate the relation between energy efficiency, spectral efficiency, and the base station density. In [20], authors study the resource allocation problem in downlink OFDMA multi-cell networks with a similar metric. Papers [19], [20] investigate the problem for homogeneous networks. On the other hand, the algorithm we proposed in this paper investigates the energy efficiency and spectral efficiency tradeoff in heterogeneous networks. Another method to combine energy efficiency and spectral efficiency metrics is to sum these metrics with appropriate weights [21]–[23]. This method is called the weighted summation model. The logarithm of the metric in the Cobb-Douglas method corresponds to the weighted summation method of the logarithms of the spectral efficiency and energy efficiency metrics. Authors in [21] investigate the energy efficiency with proportional fairness for downlink distributed antenna systems. The tradeoff between transmission power and bandwidth requirement in single-tier single-cell networks is investigated in [22]. This paper shows that the tradeoff between energy efficiency and spectral efficiency can be exploited by balancing the occupied bandwidth and power consumption. Authors in [23] propose a novel bargaining cooperative game for dense small cell networks. They show that both energy efficiency and spectral efficiency of the network can be improved with cooperation among base stations. In [23], the problem in the single-cell network is investigated. In this paper, we investigate the energy efficiency and spectral efficiency tradeoff in multi-cell multi-tier networks. We also implemented weighted summation model to combine energy efficiency and spectral efficiency metrics. In our prior work [24], we investigated the same problem. However, in [24], all resources are assigned to users during the frequency assignment process and abandoning a resource blocks is not considered. In this work, we extend our work in [24] and abandon the resource blocks depending on the network conditions.

In this paper, we study the joint maximization of energy efficiency and spectral efficiency in multi-cell heterogeneous wireless networks. The minimum rate constraints of users are addressed. The weighted summation method has been implemented to combine energy efficiency and spectral efficiency metrics. The given optimization problem is a mixture of combinatorial and non-convex optimization problems. The optimal solution requires checking all possible cell-center radii, all possible frequency allocations, and all possible power levels for all sectors in the network. Therefore, obtaining the optimum solution is extremely hard. In this paper, we propose a multi-stage algorithm whereby at each stage the solution is updated while assuming the other network conditions are constant. We show the convergence of the proposed algorithm. In the first stage, each sector selects the cell center radius that maximizes its objective function. In the second stage, the frequency resources are assigned to the users while considering the rate requirement of the users and the interference conditions of the network. In the last stage, a Levenberg-Marquardt method-based power allocation algorithm is implemented that considers the rate requirements of the users. We investigate optimal and suboptimal power updates. In the optimal approach, the Levenberg-Marquardt method-based algorithm updates all power control parameters in the sector concurrently. In the suboptimal approach, the macrocell and the low-powered base stations update their power control parameters separately. The proposed algorithm iteratively solves these three stages until convergence.

The contributions of this paper are as follows. First, we show that a Pareto optimal solution exists such that the sacrifices in terms of spectral efficiency can be transformed into gain in terms of energy efficiency or vice versa. Second, we investigate

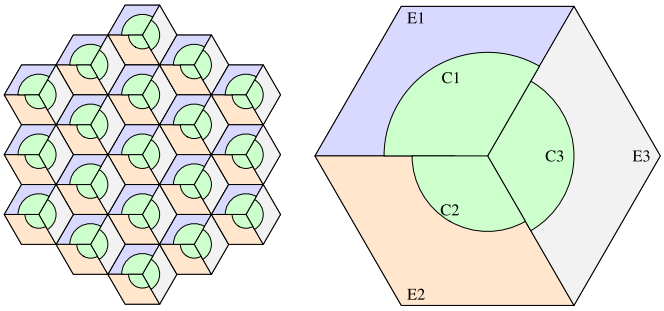

Fig. 1. Dynamic cell-center region boundaries in a multitier FFR scheme. The network layout assumes a uniform 19-cell hexagonal grid, in which the MBSs have three sector antennas and Pico-BSs employ omnidirectional antennas.

the relation between the energy efficiency and spectral efficiency tradeoff and minimum rate constraints of the users. We show that maximizing energy efficiency of the network performs better than the spectral efficiency maximization in terms of outages. Third, we show that fewer resource blocks are allocated when we increase the minimum rate constraints of users or increase the weight of the spectral efficiency in the objective metric.

The remainder of this paper is organized as follows. Section II introduces the system model, base station power consumption, and energy efficiency and spectral efficiency definitions. Section III formulates the resource allocation problem in HetNets. The proposed algorithm is presented in Section IV. Simulation results are discussed in Section V. Section VI concludes the paper.

II. System Model

In this section, we first present our system model and describe the power consumption model of the base station. Second, we define the energy efficiency and spectral efficiency metrics.

Consider a wireless network with a 19-cell hexagonal layout as depicted in Fig. 1. The edges are wrapped around to create the effect of an infinite network. In this paper, we employ the multitier FFR scheme described in [7], [8]. In each cell, one MBS is deployed along with picocell base stations (Pico-BSs). MBSs employ 3-sector antennas, whereas omnidirectional antennas are used in Pico-BSs. The overall network area is divided into 57 sectors. Each sector is divided into two regions: cell center and cell edge. In the cell-center region, macrocell associated users (MUEs) are allocated on Subband A in all sectors. On the other hand, cell-edge MUEs are allocated on Subbands B, C, or D depending on their sector. In order to limit intra-sector interference, cell-center picocell associated users (PUEs) are allocated on the remaining two subbands that the MBS does not transmit on. Cell-edge PUEs also use Subband A in addition to two subbands that cell-center PUEs are using. The transmission powers of the Pico-BSs are significantly lower than the MBSs, therefore the intra-sector interference from cell-edge Pico-BSs to cell-center MUEs will be limited. The spectrum allocation is shown in Table I.

In this paper, we study constant power allocation across the subbands. The total bandwidth of the network is divided into 4 disjoint subbands. The number of subcarriers in subbands A, B, C, and D are denoted by N_A, N_B, N_C, and N_D, respectively. The total number of subcarriers is denoted by N, i.e., $N = N_A + N_B + N_C + N_D$. In order to characterize the power assignment of base stations, we introduce two power control parameters β and ε. The parameter β is used to scale the transmission power of base stations. This parameter is defined for both MBSs and Pico-BSs. On the other hand, the parameter ε is only defined for MBSs and determines the ratio of the transmission power of MBSs on the cell-edge and the cell-center subcarriers. We can write the signal-to-interference-plus-noise ratio (SINR) of MUE k on subcarrier n as follows

$$\gamma_k^{(n)} = \frac{P_M^{(n)} g_{k,M}^{(n)}}{\sum_{\substack{M' \in \mathcal{B}_M \\ M' \neq M}} P_{M'}^{(n)} g_{k,M'}^{(n)} + \sum_{P \in \mathcal{B}_P} P_P^{(n)} g_{k,P}^{(n)} + N_0 \Delta_n} \tag{1}$$

where $P_M^{(n)}$ and $P_P^{(n)}$ are the downlink transmit powers of macrocell M and picocell P on subcarrier n, respectively. The channel gain between user k and MBS M on subcarrier n is represented as $g_{k,M}^{(n)}$. The same gain between user k and Pico-BS P is $g_{k,P}^{(n)}$. The sets of MBSs and Pico-BSs in the simulation area are denoted by $\mathcal{B}_M$ and $\mathcal{B}_P$, respectively. The bandwidth of a subcarrier n is represented by Δ_n. The thermal noise power per Hz is N_0. The SINR of PUEs can be generated by using the same approach. The downlink transmission power of MBS M for cell-center MUEs that are in sector s can be written as

$$P_M = \frac{\beta_M P_{\max,M}}{N_A^s + \varepsilon_s N_B^s}, \tag{2}$$

where $P_{\max,M}$ is the maximum transmission power of the MBS M. The numbers of assigned subcarriers on subband A and B in sector s are denoted by N_A^s and N_B^s, respectively. The downlink transmission power for cell-edge users is $\varepsilon_M P_M$. The downlink transmission power of the MBSs in other sectors can be obtained by replacing N_A^s and N_B^s with the corresponding number of subcarriers. The downlink transmission power of cell-center and cell-edge Pico-BSs in Sector 1 are denoted by P_P^C and P_P^E, and are given by

$$P_P^C = \frac{\beta_P P_{\max,P}}{N_C^s + N_D^s}, P_P^E = \frac{\beta_P P_{\max,P}}{N_A^s + N_C^s + N_D^s}. \tag{3}$$

The numbers of assigned subcarriers on subband C and D in sector s are denoted by N_C^s and N_D^s, respectively. For the Pico-BSs in other sectors, the transmission power can be calculated similarly, by replacing N_A^s, N_C^s, and N_D^s with the corresponding number of subcarriers.

Consider sector s to consist of $K_{M,s}$ MUEs and $K_{P,s}$ PUEs. The sets of MUEs and PUEs are denoted by $\mathcal{K}_{M,s}$ and $\mathcal{K}_{P,s}$, respectively. We use index k for user k and index n for subcarrier n. We define vector $\boldsymbol{C}_{M,s}$ to show whether MUE is in the cell center or not. The size of this vector is $K_{M,s}$. If an MUE k is located in the cell center, $\boldsymbol{C}_{M,s}^k = 1$, otherwise $\boldsymbol{C}_{M,s}^k = 0$. Likewise, the vector $\boldsymbol{C}_{P,s}$ denotes whether PUE is in cell center or not. The size of $\boldsymbol{C}_{P,s}$ is $K_{P,s}$. If PUE k is located in the cell center, $\boldsymbol{C}_{P,s}^k = 1$, otherwise $\boldsymbol{C}_{P,s}^k = 0$. The matrices $\boldsymbol{F}_{M,s}$ and $\boldsymbol{F}_{P,s}$ denote whether the subcarrier n is assigned to user k or

TABLE I
SPECTRUM ASSIGNMENT IN A MULTITIER FFR SCHEME

Base Station Type	Sector 1		Sector 2		Sector 3	
	Cell-Center(C1)	Cell-Edge(E1)	Cell-Center(C2)	Cell-Edge(E2)	Cell-Center(C3)	Cell-Edge(E3)
MBS	A	B	A	C	A	D
Pico-BS	C and D	A, C, and D	B and D	A, B, and D	B and C	A, B, and C

not. The size of the matrices $\boldsymbol{F}_{M,s}$ and $\boldsymbol{F}_{P,s}$ are $K_{M,s} \times N$ and $K_{P,s} \times N$, respectively. If the subcarrier n is assigned to MUE k, the (n,k)th element of $\boldsymbol{F}_{M,s}$ will be 1, otherwise it will be 0. The same approach is used for frequency allocation of $\boldsymbol{F}_{P,s}$. The matrices $\boldsymbol{R}_1$ and $\boldsymbol{R}_2$ denote the throughput of MUEs. The size of these matrices are $N \times K_{M,s}$. The (n,k)th element of matrix $\boldsymbol{R}_1$ is the throughput of MUE k on subcarrier n when MUE k is in the cell-center region. The same element of $\boldsymbol{R}_2$ corresponds to the same value when the user is located in the cell-edge region. The matrices $\boldsymbol{R}_3$ and $\boldsymbol{R}_4$ consist of the throughput of PUEs. The size of these matrices are $N \times K_{P,s}$. The (n,k)th element of $\boldsymbol{R}_3$ and $\boldsymbol{R}_4$ is the throughput of PUE k on subcarrier n when the user is in cell center and cell edge, respectively. Then, we can calculate the aggregate throughput of the sector s as

$$R_s = \sum_{k \in \mathcal{K}_{M,s}} \left(\boldsymbol{C}^k_{M,s} \boldsymbol{F}^{(k,:)}_{M,s} \boldsymbol{R}^{(:,k)}_1 + (1 - \boldsymbol{C}^k_{M,s}) \boldsymbol{F}^{(k,:)}_{M,s} \boldsymbol{R}^{(:,k)}_2 \right) + \sum_{k \in \mathcal{K}_{P,s}} \left(\boldsymbol{C}^k_{P,s} \boldsymbol{F}^{(k,:)}_{P,s} \boldsymbol{R}^{(:,k)}_3 + (1 - \boldsymbol{C}^k_{P,s}) \boldsymbol{F}^{(k,:)}_{P,s} \boldsymbol{R}^{(:,k)}_4 \right). \tag{4}$$

Note that $\boldsymbol{X}^{(n,:)}$ and $\boldsymbol{X}^{(:,k)}$ are the nth row vector of the matrix $\boldsymbol{X}$ and the kth column vector of the matrix $\boldsymbol{X}$, respectively. The throughput terms in (4) can be expanded by using the definitions in (1) as

$$\boldsymbol{R}^{(n,k)}_i = \Delta_n \log_2 \left(1 + \gamma^{(n)}_k \right), \quad \text{for all } i \in 1,2,3,4, \tag{5}$$

where $\boldsymbol{X}^{(n,k)}$ is the entry on the nth row and kth column of the matrix $\boldsymbol{X}$.

A. Base Station Power Consumption Models

Modeling the energy consumption of the base stations has attracted some attention in the literature, see, e.g., [25]–[27]. Several components contribute to the energy consumption of the base stations such as power amplifier, power supply, cooling device, etc. A good model must include the contribution of all components. In order to quantify the energy savings properly, a load-dependent model is required. In this paper, we use the power consumption model that is described in [25]. In this model, the power consumption of the base station is broken down into two parts: load-dependent and static power consumption. The load-dependent part changes depending on the transmission power of the base station. On the other hand, static power is independent of the transmission power and it will be consumed if the base station is on. If the base station has no user to serve, then it goes into the sleep mode. During the sleep mode, energy consumption of the base station is lower than the static power consumption of the base station. This model is given by

$$P_{Total} = \begin{cases} N_{TRX} \left(P_0 + \Delta \cdot P_{TX} \right) & 0 < P_{TX} \leq P_{\max} \\ N_{TRX} P_{sleep} & P_{out} = 0 \end{cases} \tag{6}$$

where P_{Total}, P_{TX}, and P_{sleep} are the overall power consumption of the base station, load-dependent transmission power, and the power consumption during the sleep mode. The maximum transmission power of the base station is denoted by $P_{\max}$. The number of the transceiver chains is represented by N_{TRX}. The slope of the load-dependent power consumption is Δ. By using this model, the power consumption of the MBSs and Pico-BSs can be written as

$$\begin{aligned} P_M &= N_{TRX,M} \left(P_{0,M} + \Delta_M P_{TX,M} \right) \text{ and} \\ P_P &= N_{TRX,P} \left(P_{0,P} + \Delta_P P_{TX,P} \right) \end{aligned} \tag{7}$$

where P_M and P_P denote the overall power consumption of MBS M and Pico-BS P, respectively. The parameters $P_{0,M}$ and $P_{0,P}$ are the static power consumption at MBS M and Pico-BS P, respectively. The transmission power of the MBS M and Pico-BS P are denoted by $P_{TX,M}$ and $P_{TX,P}$, respectively. The numbers of transceiver chains for MBS M and Pico-BS P are represented by $N_{TRX,M}$ and $N_{TRX,P}$, respectively. The slopes of the power consumption for MBS M and Pico-BS P are denoted by Δ_M and Δ_P, respectively. If no user is associated with a base station, the corresponding base stations go into sleep mode. The power consumptions of the MBS M and Pico-BS P during the sleep mode are denoted by $P_{sleep,M}$ and $P_{sleep,P}$, respectively.

B. Energy Efficiency and Spectral Efficiency Definition

Let η_s denote the energy efficiency of sector s which can be expressed as

$$\eta_s(\boldsymbol{\varepsilon}, \boldsymbol{\beta}) = \frac{R_s}{\psi_s(\varepsilon_s, \boldsymbol{\beta}_s)}, \tag{8}$$

where the vectors $\boldsymbol{\varepsilon}$ and $\boldsymbol{\beta}$ denote the optimization variables of transmission power for all sectors in the network. The scalar parameter ε_s is the ε value of the sector s. The vector $\boldsymbol{\beta}_s$ consists of all β values of the base stations in sector s. The total power consumption in sector s is denoted by $\psi_s(\varepsilon_s, \boldsymbol{\beta}_s)$ which can be calculated as

$$\psi_s(\varepsilon_s, \boldsymbol{\beta}_s) = P_M + \sum_{P \in \mathcal{N}_{\text{Pico},s}} P_P, \tag{9}$$

where $\mathcal{N}_{\text{Pico},s}$ is the set of Pico-BSs in sector s. Thus, the energy efficiency $\eta_s(\boldsymbol{\varepsilon}, \boldsymbol{\beta})$ has the unit bits/Joule.

In the same fashion, we can calculate the spectral efficiency of the sector s as follows

$$\nu_s(\boldsymbol{\varepsilon}, \boldsymbol{\beta}) = \frac{R_s}{W_s}, \tag{10}$$

where W_s is the total bandwidth allocated by MBS and Pico-BSs in sector s. The unit of $\nu_s(\boldsymbol{\varepsilon}, \boldsymbol{\beta})$ is bits/s/Hz.

III. Problem Formulation

In this section, we develop a framework to investigate energy efficiency and spectral efficiency tradeoff in multi-cell heterogeneous networks. Our objective is to maximize both energy efficiency and spectral efficiency of the network while satisfying the minimum rate requirements of users. As stated earlier, the problems of maximizing energy efficiency and spectral efficiency of the network usually contradict with each other. Therefore, we introduce a multi-objective optimization-based formulation to maximize energy efficiency and spectral efficiency simultaneously. Multi-objective problems are usually solved by combining objectives under a single objective. In that manner, we use the weighted summation method to combine the energy efficiency and spectral efficiency metrics. However, the units of these metrics are not the same. The unit of energy efficiency is bits/Joule and the unit of spectral efficiency is bits/s/Hz. To ensure the units of these metrics are the same in weighted summation form, we multiply the spectral efficiency function with W_{tot}/P_s. The parameter W_{tot} is the total bandwidth of the network and P_s is the total amount of power consumption of sector s when all BSs in this sector transmit at the full power. A similar approach is also used in [22]. In addition, we introduce the unitless parameter α, $0 \leq \alpha \leq 1$, to tune the objective metric. This parameter helps us tune the network towards energy efficiency or spectral efficiency depending on the network conditions. During the peak hours, increasing spectral efficiency is more important than the energy efficiency to satisfy the demand of more users. On the other hand, during the off-peak hours, maximizing energy efficiency becomes more important to decrease the energy consumption of the network. The objective metric moves towards spectral efficiency when parameter α increases. On one extreme, when α is 1, the problem becomes spectral efficiency maximization; on the other extreme, when α is 0, the problem is energy efficiency maximization. Thus, α allows a service provider to make a judicious decision between the two efficiency measures depending on their own criteria. In addition, for constant α, when we increase W_{tot}, the weight of the spectral efficiency function increases in the objective function. When there is sufficient bandwidth, the objective function emphasis is on saving more bandwidth and maximizing the efficiency of the occupied bandwidth. On the other hand, if we have sufficient power, the importance of the energy efficiency in the objective function increases. A multi-objective optimization problem employing the variables we specified above can be defined as follows

$$\max_{\boldsymbol{\beta},\boldsymbol{\varepsilon},\mathbf{C},\mathbf{F}} \sum_{s\in\mathcal{S}} (1-\alpha)\eta_s(\boldsymbol{\varepsilon},\boldsymbol{\beta}) + \alpha\frac{W_{tot}}{P_s}\nu_s(\boldsymbol{\varepsilon},\boldsymbol{\beta})$$

$$\text{s.t. } \boldsymbol{C}^k_{M,s}\boldsymbol{F}^{(k,:)}_{M,s}\boldsymbol{R}^{(:,k)}_1 + (1-\boldsymbol{C}^k_{M,s})\boldsymbol{F}^{(k,:)}_{M,s}\boldsymbol{R}^{(:,k)}_2 \geq R_{\min,k}, \text{for all } k \in \mathcal{K}_{M,s}, s \in \mathcal{S} \tag{11a}$$

$$\text{s.t. } \boldsymbol{C}^k_{M,s}\boldsymbol{F}^{(k,:)}_{M,s}\boldsymbol{R}^{(:,k)}_3 + (1-\boldsymbol{C}^k_{M,s})\boldsymbol{F}^{(k,:)}_{M,s}\boldsymbol{R}^{(:,k)}_4 \geq R_{\min,k}, \text{for all } k \in \mathcal{K}_{P,s}, s \in \mathcal{S} \tag{11b}$$

$$\sum_{\substack{k\in\mathcal{K}_{M,s}\\ \boldsymbol{C}^k_{M,s}=1}} \boldsymbol{F}^{(k,n)}_{M,s} \leq 1 \text{ and } \sum_{\substack{k\in\mathcal{K}_{M,s}\\ \boldsymbol{C}^k_{M,s}=0}} \boldsymbol{F}^{(k,n)}_{M,s} = 0 \quad \text{for all } n \in \mathcal{N}^C_{M,s}, s \in \mathcal{S} \tag{11c}$$

$$\sum_{\substack{k\in\mathcal{K}_{M,s}\\ \boldsymbol{C}^k_{M,s}=0}} \boldsymbol{F}^{(k,n)}_{M,s} \leq 1 \text{ and } \sum_{\substack{k\in\mathcal{K}_{M,s}\\ \boldsymbol{C}^k_{M,s}=1}} \boldsymbol{F}^{(k,n)}_{M,s} = 0 \quad \text{for all } n \in \mathcal{N}^E_{M,s}, s \in \mathcal{S} \tag{11d}$$

$$\sum_{k\in\mathcal{K}_{M,s}} \boldsymbol{F}^{(k,n)}_{M,s} = 0 \quad \text{for all } n \notin \mathcal{N}^C_{M,s} \cup \mathcal{N}^E_{M,s}, s \in \mathcal{S} \tag{11e}$$

$$\sum_{\substack{k\in\mathcal{K}^p_{P,s}\\ \boldsymbol{C}^k_{P,s}=1}} \boldsymbol{F}^{(k,n)}_{P,s} \leq 1 \text{ and } \sum_{\substack{k\in\mathcal{K}^p_{P,s}\\ \boldsymbol{C}^k_{P,s}=0}} \boldsymbol{F}^{(k,n)}_{P,s} = 0 \quad \text{for all } n \in \mathcal{N}^C_{P,s}, p \in \mathcal{N}_{Pico,s}, s \in \mathcal{S} \tag{11f}$$

$$\sum_{\substack{k\in\mathcal{K}^p_{P,s}\\ \boldsymbol{C}^k_{P,s}=0}} \boldsymbol{F}^{(k,n)}_{P,s} \leq 1 \text{ and } \sum_{\substack{k\in\mathcal{K}^p_{P,s}\\ \boldsymbol{C}^k_{P,s}=1}} \boldsymbol{F}^{(k,n)}_{P,s} = 0 \quad \text{for all } n \in \mathcal{N}^E_{P,s}, p \in \mathcal{N}_{Pico,s}, s \in \mathcal{S} \tag{11g}$$

$$\sum_{k\in\mathcal{K}^p_{P,s}} \boldsymbol{F}^{(k,n)}_{P,s} = 0 \quad \text{for all } n \notin \mathcal{N}^C_{P,s} \cup \mathcal{N}^E_{P,s}, \; p \in \mathcal{N}_{Pico,s}, s \in \mathcal{S} \tag{11h}$$

$$\boldsymbol{\varepsilon} \succeq \mathbf{0} \text{ and } \mathbf{0} \preceq \boldsymbol{\beta} \preceq \mathbf{1}, \tag{11i}$$

where $\mathcal{S}$ is the set of all sectors in the simulation area. The minimum rate requirement of user k is denoted by $R_{\min,k}$. The parameters $\mathcal{N}^C_{M,s}$ and $\mathcal{N}^E_{M,s}$ are the set of subcarriers that are assigned to cell-center and cell-edge MUEs, respectively. Likewise, the parameters $\mathcal{N}^C_{P,s}$ and $\mathcal{N}^E_{P,s}$ are the set of subcarriers that are assigned to cell-center and cell-edge PUEs, respectively. The notation $\mathbf{x} \succeq \mathbf{0}$ forces that each element of vector $\mathbf{x}$ is greater than or equal to 0. Constraints (11a) and (11b) ensure that rate constraints of the MUEs and PUEs are satisfied, respectively. Constraints (11c) to (11h) guarantee that available resources to a base station for a region are assigned to users that are associated with the base station and in the corresponding region and unavailable resources are not assigned to these users. Constraint (11i) guarantees that parameters $\boldsymbol{\varepsilon}$ and $\boldsymbol{\beta}$ are within the given limits.

The objective function in (11) is non-convex, therefore the optimal solution requires exhaustive search over all possible cell-center radii, frequency assignments, and power levels for all sectors. To tackle this problem, we divide our problem into $|S|$ subproblems so that each sector maximizes its own objective function simultaneously. This resource allocation problem still needs to be solved over the cell-center radius, frequency, and power domains jointly. This problem is combinatorial over the first two domains and non-convex over the power allocation domain [28], [29]. Therefore, obtaining the optimum solution still requires exhaustive search over all domains. Therefore, instead of solving these problems jointly, we propose a three-stage algorithm that solves each problem consecutively. In the next section, we will describe these stages and discuss the complexity and convergence analysis of the proposed algorithm.

IV. Proposed Solution

Our formulation in (11) enables us to develop an energy- and spectral-efficient resource allocation algorithm. We first divide the problem in (11) into $|S|$ subproblems such that each sector maximizes own objective function. Then, the proposed algorithm decouples the problem into three stages and solves them iteratively until convergence. In the first stage, we select the cell-center radius to divide MUEs into two groups as cell-center MUEs and cell-edge MUEs and also determine the available resources to the Pico-BSs depending on their regions. Second, MBS and Pico-BSs assign frequency resources to their users. This stage has two steps. In the first step, MBS and Pico-BSs assign the resource blocks to their users to maximize the objective metric and satisfy the rate requirements of their users. In the second step, the MBS and all Pico-BSs in the sector make a judicious decision to maximize the overall objective among the following: abandon one of the assigned resource block from all base stations, allocate one more resource block among the available ones, or protect the current allocation. By this approach, the available resources to each sector are updated in each iteration until the optimum allocation is found. Last, we determine the power control parameters ε and β s in each sector concurrently. The minimum rate requirements of the users are included in the power control subproblem by using dual decomposition techniques. After these three stages, the MBS sends the updated information to the other base stations in the network. Then, these stages are repeated in every sector until convergence. The proposed algorithm is presented under the heading Algorithm 1. The flowchart of this algorithm is depicted in Fig. 2. In the sequel, we discuss each step of the proposed algorithm in detail.

A. The Cell-Center Region Boundaries

In the first stage of the proposed algorithm, we need to set the cell-center region boundaries in each sector to select the region of the MUEs and also determine the available resources to Pico-BSs. In [8], we showed that more than two times gain can be obtained in terms of energy efficiency and throughput by proper selection of cell-center radii. In [8], we proposed two cell-center radius selection algorithms. The first algorithm selects a cell-center radius to maximize the throughput of the sector. The second algorithm aims to distribute resources evenly among MUEs. However, neither of these algorithms considers the minimum rate requirements of users. For example, when the minimum rate requirements of users are low, the first algorithm is preferable over the second one to maximize the objective metric. On the other hand, if users have higher rate requirements, the second algorithm should be selected over the first one to satisfy the rate requirements of more users. Therefore, in order to benefit from the advantages of both algorithms, we propose a dynamic cell-center selection algorithm in this paper. First, we will provide a useful observation.

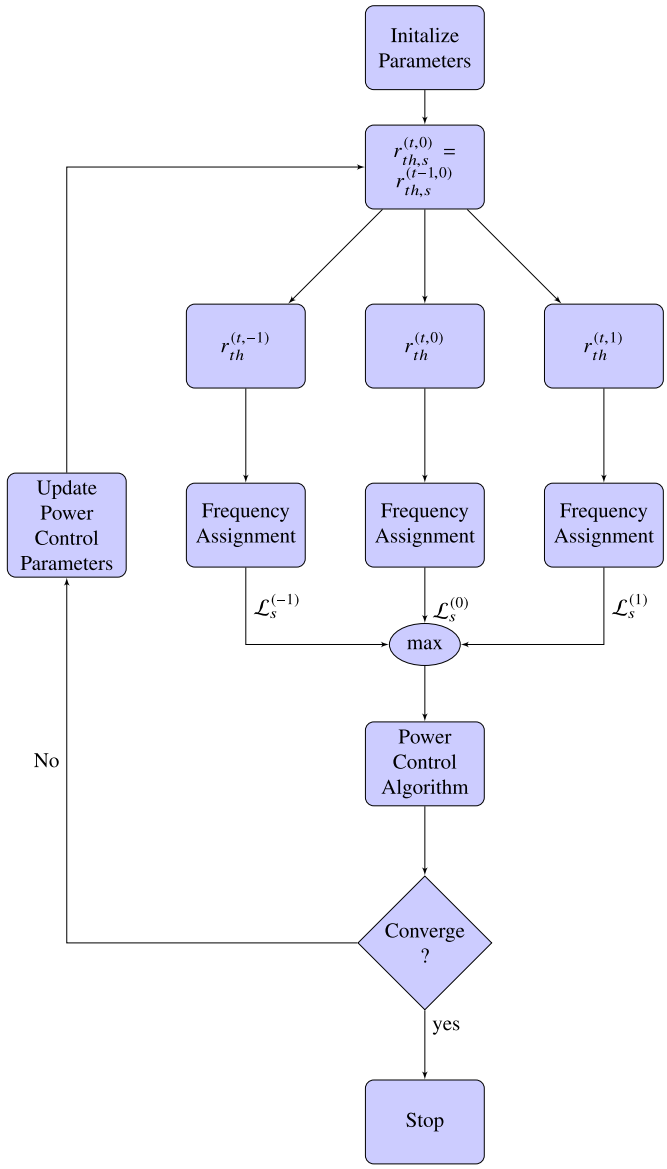

Fig. 2. Flowchart of the proposed algorithm in Algorithm 1.

Observation 1: The resource distribution of the FFR scheme changes only when one of the cell-center MUEs or cell-center Pico-BSs passes to the cell-edge region or vice versa.

When we expand or shrink the cell-center radius without changing the region of an MUE or a Pico-BS, the region of all users and Pico-BSs will be the same. Therefore, the solution of

Algorithm 1: Proposed Energy- and Spectral-Efficient Resource Allocation Algorithm.

1: **Initialize:** $r_{th,s}^{(0,c)} = r_{r,s}/2 \quad (\varepsilon_s^{(0)}, \boldsymbol{\beta}_s^0) = [1, \mathbf{1}]$
2: $r_{th,s}^{(t,0)} = r_{th,s}^{(t-1,0)}$
3: First, three-candidate cell-center region boundaries are selected by using the cell-center radius algorithm in Section IV-A: $r_{th,s}^{(t,-1)}$, $r_{th,s}^{(t,0)}$, and $r_{th,s}^{(t,1)}$.
4: $r_{th,s}^{(t,0)} = r_{th,s}^{(t-1,0)}$. The cell-center radius $r_{th,s}^{(t,-1)}$ is obtained by shrinking $r_{th,s}^{(t,0)}$, and $r_{th,s}^{(t,1)}$ is obtained by expanding $r_{th,s}^{(t,c)}$.
5: **for** $c := -1$ to 1 **do**
6: For cell-center radius, $r_{th,s}^{(t,c)}$, run the frequency assignment algorithm in Section IV-B for each base station in the sector.
7: Calculate the Lagrangian functions, $\mathcal{L}_s^{(c)}$, which is described in the Section IV-C.
8: Note that while calculating the Lagrangian function, power control parameters that are obtained at the end of the previous time instant are used.
9: **end for**
10: Among all three Lagrangian function, the maximum one is selected for the cell-center radius and the frequency assignments.
11: Then, run the power control algorithm that is described in Section IV-C to determine the power control parameters.
12: Go to Step 1 and repeat until the convergence.

the frequency assignment and power assignment problems will be the same.

Therefore, $K_{M,s} + N_{\text{Pico},s} + 1$ different cell-center radii can be selected for sector s. When the number of users in the sector or the number of pico-BSs in the sector increases, exhaustive search over all radii requires a significant amount of time. In addition, the frequency assignment problem that will be discussed in the next subsection needs to be solved for every radius option. Therefore, we need to eliminate some of these radii choices judiciously. In this paper, we propose an iterative algorithm for cell-center radius selection. The proposed algorithm compares the Lagrangian function of the current cell-center radius with two cell-center radii: one more MUE or Pico-BS is included in the cell-center region from the cell-edge region and one more MUE or Pico-BS is excluded to the cell-edge region from the cell-center region. Among these three cell-center radii, the one that maximizes the Lagrangian function is selected as the cell-center radius. This approach decreases the number of cell-center radii that will be checked in every iteration from $K_{M,s} + N_{\text{Pico},s} + 1$ to three. Therefore, a significant amount of time will be saved by this approach. We used a similar algorithm in our prior work [9].

B. Frequency Assignment Problem

In the second stage of the algorithm, frequency resources are assigned to users. In the literature, several scheduling algorithms are discussed, see, e.g., [30]. Each scheduler has its own priorities such as minimizing latency, maximizing fairness, etc. In [28], it is shown that the optimal resource allocation among $K_{M,s}$ users and $N_{M,s}^C$ resource blocks requires $K_{M,s}^{N_{M,s}^C}$ searches. This approach is impractical in real time applications. Therefore, we propose a two-step opportunistic scheduling algorithm in this paper. Before discussing the proposed scheduling algorithm, we will provide some useful theorems.

Theorem 1: The power consumption of a base station is minimized when the maximum of $R_{\min,k}/R_{curr,k}$, R_{ratio}, is minimized where $R_{curr,k}$ is the current rate of user k when no power control is implemented.

Proof: Let us compare two different cases of scheduling that consume equal amount of power. Assume the minimum rate requirements of all users is satisfied with the current power assignment and R_{ratio}^1 is bigger than R_{ratio}^2, i.e., $1 > R_{ratio}^1 > R_{ratio}^2$. The power control algorithm that minimizes the power consumption will increase both ratios to 1. While the total power consumption of the first case is $R_{ratio}^1 \cdot P$, that of the second case will be $R_{ratio}^2 \cdot P$. Therefore, less power will be consumed in the second case than the first case. ■

Theorem 2: The spectral efficiency of the resource block is maximized when a resource block is assigned to a user that has the best average channel gain over the subcarriers of the resource block.

Proof: The proof of this theorem is straightforward. When a user has the best average channel gain over the subcarriers of the resource block, it has the highest capacity. Due to the fact that the total bandwidth of the resource block will be the same for all users, the user who has the highest channel gain will also provide the highest spectral efficiency for that resource block. ■

The proposed scheduling algorithm has two steps. In the first step, the available resource blocks are assigned to users. The proposed algorithm assigns the resource blocks to users iteratively. In each iteration, one resource block is assigned to a user. Our priority is satisfying the minimum rate requirements of more users. For this purpose, if there are users that could not satisfy their rate requirement with the current assignment, assigning a resource block to one of these users is the most judicious choice. In order to maximize our objective, we assign the resource block to the user that provides the largest improvement in terms of the Lagrangian function among the users that could not satisfy their rate requirement. If all users satisfy their rate requirement with the current assignment, available resource blocks are assigned to the user that provides the largest Lagrangian improvement among all users. By this approach, first, the rate requirement of more users are satisfied. Second, the power consumption of the network is minimized. Third, the spectral efficiency of the network is maximized. During this step, power allocations in the previous time instant are used to calculate the rates of the users with the current assignment. In the second step of the algorithm, all base stations in a sector determine whether to protect the current assignment, abandon one resource block, or assign one more resource block among the available but unassigned ones. When a resource block is not allocated by any user in a sector, the intercell interference to users in the other

sector is lowered which increases the utility function of the other sectors. In addition, fewer resource blocks are assigned by base stations in the sector, therefore power assignment of other resource blocks increases. This may also increase the spectral efficiency of the sector. In the next section, we present the two steps of the opportunistic scheduling algorithm and then discuss the complexity of the algorithm.

Opportunistic Scheduler Algorithm: The opportunistic scheduler algorithm shares resource blocks among users to maximize the objective metric. Due to the fact that the cell-center and cell-edge MUEs are allocated different subbands, this algorithm runs for both sets separately. First, the proposed algorithm assigns a resource block to a user that provides maximum improvement to the Lagrangian function that is described in Section IV-C. If the rate requirement of the corresponding user is satisfied with the current assignment, this user is removed from the assignment set. The proposed algorithm continues to allocate resource blocks to users in the assignment set. If the minimum rate requirements of all users are satisfied with the current assignment (i.e., the assignment set is empty), the proposed algorithm assigns the rest of the available resource blocks to users that provide the largest Lagrangian improvement. The resource allocation algorithm for cell-center MUEs is given under the heading Algorithm 2. The same approach can be used for the cell-edge MUEs and Pico-BSs.

Due to the interference conditions in the network, not assigning a resource block to any user in the sector may improve the overall utility of the network. In addition, when a resource block is not assigned by all base stations in a sector, the denominator of the spectral efficiency function becomes smaller that may also improve the spectral efficiency of the sector. In order to benefit from these properties, we decide among the following three cases in each iteration: abandoning one of the resource blocks from all base stations, allocating one more resource block among the available ones, or protecting the current situation. For each resource block, we calculate the utility function without assigning this resource block. In addition, for each unassigned but available resource block, we calculate the utility function when this resource block is assigned. Among all these cases the one that has the largest Lagrangian function is selected as the current frequency resource allocation.

1) Complexity Analysis: In the first step of the scheduling algorithm, each base station calculates the rate of each available resource block for each user in the sector. Therefore, the complexity of the first step is $\mathcal{O}(NK)$ for each base station when there are N resource blocks to assign to K users. In the second step, the complexity of the algorithm is different for MBSs and Pico-BSs. In MBSs, the rate of each resource block is required to be recalculated for one more resource block assignment and one more resource block abandonment. When we look at the formula in (2), abandoning or assigning a cell-center resource block and cell-edge resource block has affected the downlink transmission power of the MBS differently. Therefore, we have to calculate different rates for all these cases. In the first step, the resource blocks are already assigned to users, therefore we have to calculate the rate of each resource block for these four cases. The complexity of this process becomes $\mathcal{O}(4N)$. On the other hand, the effect of abandoning or assigning a resource block from different subbands on the downlink transmission power will be the same. Therefore, the complexity of this process at Pico-BSs is $\mathcal{O}(2N)$.

Algorithm 2: Proposed Frequency Allocation Algorithm.

Initialize: $\boldsymbol{F}_{M,s} = \mathbf{0}$
$\mathcal{N}_{M,s}^{C,t} = \mathcal{N}_{M,s}^{C,t-1}$. $\mathcal{N}_{M,s}^{C,t-1}$ is the frequency resources that are assigned at time instant $t-1$
$\mathcal{K}_{M,s}^{C,U} = \mathcal{K}_{M,s}^{C}$
while $\mathcal{N}_{M,s}^{C,t}$ and $\mathcal{K}_{M,s}^{C,U}$ are not empty **do**
  $k = \arg\max_{k \in \mathcal{K}_{M,s}^{C,U}} \mathcal{L}_s^{(C,k,n)}$
  $\boldsymbol{F}_{M,s}^{(k,n)} = 1$
  if $\boldsymbol{F}_{M,s}^{(k,:)} \boldsymbol{R}_1^{(:,k)} \geq R_{\min,k}$ **then**
    $\mathcal{K}_{M,s}^{C} \longleftarrow \mathcal{K}_{M,s}^{C} \backslash k$
  end if
  $\mathcal{N}_{M,s}^{C,t-1} \longleftarrow \mathcal{N}_{M,s}^{C,t} \backslash n$
end while
while $\mathcal{N}_{M,s}^{C,t}$ is not empty **do**
  $k = \arg\max_{k \in \mathcal{K}_{M,s}^{C}} \mathcal{L}_s^{(C,k,n)}$
  $\boldsymbol{F}_{M,s}^{(k,n)} = 1$
  $\mathcal{N}_{M,s}^{C,t-1} \longleftarrow \mathcal{N}_{M,s}^{C,t} \backslash n$
end while

C. Power Control Problem

In the third stage of the algorithm, we determine the power levels on each subband that maximize our objective metric and also satisfy the rate requirements of the users. Given the cell-center radius vector and the frequency assignment matrix, we need to determine the power control parameters $\boldsymbol{\beta}_s$ and ε_s. We use convex optimization techniques to obtain optimum $\boldsymbol{\beta}$ and ε parameters.

Lemma 1: The energy efficiency and spectral efficiency per sector expression $(1-\alpha)\eta_s(\boldsymbol{\varepsilon}, \boldsymbol{\beta}) + \alpha \frac{W_{tot}}{P_s} \nu_s(\boldsymbol{\varepsilon}, \boldsymbol{\beta})$ in (11) is quasiconcave in ε_s and $\boldsymbol{\beta}_s$.

Proof: The proof is given in the online Appendix [31].

During obtaining optimum power control parameters, we assume that the power control parameters of the other sectors are constant. Therefore, the interference conditions from the other sectors are assumed to be constant. However, if the base stations increase their transmission powers to high levels without considering the other sector, this harms the transmissions in other sectors and causes outages and decrease in the overall utility. To prevent this, we introduce the interference pricing mechanism. Several pricing algorithms are discussed in the literature. In [10] and [32], each base station is penalized with the transmission power level of the base station. The penalty term is a constant term times the transmission power level of the base station. Although this approach forces the base stations to decrease their transmission power, the penalty term will be independent of the interference that the base stations create. Therefore, the

improvement in overall network utility may not reach its actual potential. For this reason, we use an interference-based pricing mechanism in this paper. The pricing mechanism penalizes each sector by the amount of the interference it creates. This approach was first proposed in [11]–[13]. We use $\theta_s(\varepsilon_s, \boldsymbol{\beta}_s)$ to denote the interference pricing function for sector s. The interference pricing function proportionally increases with the interference that the base station creates. In addition, if the interference causes the outages of users in other sectors, the penalty term becomes more severe.

Section IV-B guarantees that constraints (11c)–(11h) are satisfied for each base station. In addition, when the minimum rate requirement of the users increases, some users may not be allocated any resources to decrease the overall outage probabilities of the network. When this is the case, the minimum rate requirement of these users cannot be satisfied with the power control algorithm. Therefore, we exclude these users from the power control problem and define sets of MUEs and PUEs that are assigned to at least one resource block as $\mathcal{K}^U_{M,s}$ and $\mathcal{K}^U_{P,s}$, respectively. When we write the Lagrangian of the problem (11) for the remaining constraints and users, we obtain

$$\begin{aligned}\mathcal{L}_s(\mathbf{x}_s) = {} & (1-\alpha)\eta_s(\boldsymbol{\varepsilon},\boldsymbol{\beta}) + \alpha\frac{W_{tot}}{P_s}\nu_s(\boldsymbol{\varepsilon},\boldsymbol{\beta}) - \theta_s(\varepsilon_s,\boldsymbol{\beta_s}) \\ & - \sum_{k\in\mathcal{K}^U_{M,s}} \lambda_{k,s}\Big(R_{\min,k} - \Big(\boldsymbol{C}^k_{M,s}\boldsymbol{F}^{(k,:)}_{M,s}\boldsymbol{R}^{(:,k)}_1 \\ & + (1-\boldsymbol{C}^k_{M,s})\boldsymbol{F}^{(k,:)}_{M,s}\boldsymbol{R}^{(:,k)}_2\Big)\Big) + \sum_{k\in\mathcal{K}^U_{P,s}} \lambda_{k,s}\Big(R_{\min,k} \\ & - \Big(\boldsymbol{C}^k_{M,s}\boldsymbol{F}^{(k,:)}_{M,s}\boldsymbol{R}^{(:,k)}_3 + (1-\boldsymbol{C}^k_{M,s})\boldsymbol{F}^{(k,:)}_{M,s}\boldsymbol{R}^{(:,k)}_4\Big)\Big) \\ & + \tau^L_M\beta_M + \tau^U_M(1-\beta_M) + \sum_{P\in\mathcal{N}_{\text{Pico},s}} \tau^L_P\beta_P \\ & + \sum_{P\in\mathcal{N}_{\text{Pico},s}} \tau^U_P(1-\beta_P) + \rho_s\varepsilon_M. \end{aligned} \tag{12}$$

For simplicity, we will use $\mathcal{L}_s(\mathbf{x}_s)$ for $\mathcal{L}(\varepsilon_s, \boldsymbol{\beta}_s, \boldsymbol{\lambda}, \boldsymbol{\tau^L}_s, \boldsymbol{\tau^U}_s, \rho_s)$ throughout the rest of the paper.

In this paper, the transmission power of the MBS M depends on β_M and ε_M and the transmission power of the Pico-BS P depends on β_P. The interference pricing function accounts for the interference that all base stations in the sector s are subject to. We define a vector, $\mathbf{z}_s = [\beta_M\,\varepsilon_M\,\beta^1_P \ldots \beta^{N_{P,s}}_P]$ where $N_{P,s}$ is the number of Pico-BSs in sector s. Then, we can write the interference pricing function as follows

$$\theta_s(\varepsilon_s, \boldsymbol{\beta}_s) = \mathbf{z}^T_s \sum_{\substack{s'\in\mathcal{S}\\ s'\neq s}} \nabla_{\mathbf{z}_s}\mathcal{L}_{s'}(\mathbf{x}_{s'}). \tag{13}$$

The pricing function reflects the marginal costs of the variables β_M, ε_M, and β_P s for all Pico-BSs.

In each sector, there are $2 + N_{Picos}$ power control parameters. In order to obtain the optimum power control parameters, we will employ the Levenberg-Marquardt method. The Levenberg-Marquardt method is a variant of the Newton method. The Newton method provides quadratic convergence. The quadratic approximation of the Lagrangian function in (12) can be expressed as

$$\begin{aligned} g(\mathbf{z}) = {} & \mathcal{L}_s(\mathbf{x}_s) + \nabla\mathcal{L}_s(\mathbf{x}_s)^T\big(\mathbf{z} - \mathbf{z}^{(t,l)}_s\big) \\ & + \frac{1}{2}\big(\mathbf{z} - \mathbf{z}^{(t,l)}_s\big)^T\nabla^2\mathcal{L}_s(\mathbf{x}_s)(\mathbf{z} - \mathbf{z}^{(t,l)}_s), \end{aligned} \tag{14}$$

where l and t denote the Newton iteration and time instant, respectively. The Hessian matrix of the $\mathcal{L}_s(\mathbf{x}_s)$ at $\mathbf{z}^{(t,l)}_s$ is denoted by $\nabla^2\mathcal{L}_s(\mathbf{x}_s)$. However, the Newton method does not guarantee convergence [33]. The reason behind this is that the Hessian matrix can be singular or the direction may not be correct. In order to overcome this problem, several methods have been investigated in the literature [33], [34]. In this paper, we employ the Levenberg-Marquardt method due to its guarantee of convergence. Then, the power control parameters that maximize $g(\mathbf{z})$ can be obtained by

$$\mathbf{z}^{(t,l+1)}_s = \mathbf{z}^{(t,l)}_s - \mu_l\big(\nabla^2\mathcal{L}^{(l)}_s(\mathbf{x}_s) - \xi\mathbf{I}\big)^{-1}\nabla\mathcal{L}^{(l)}_s(\mathbf{x}_s), \tag{15}$$

where $\mathbf{I}$ is the identity matrix. The term $\xi\mathbf{I}$ should be selected in such a way that all the eigenvalues of $\mathbf{D} = (\nabla^2\mathcal{L}^{(l)}_s(\mathbf{x}_s) - \xi\mathbf{I})$ are negative. This approach guarantees that $\mathbf{D}$ is negative definite. The parameter ξ should be selected larger than the highest positive eigenvalue of the $\nabla^2\mathcal{L}^{(l)}_s(\mathbf{x}_s)$. If all eigenvalues of $\nabla^2\mathcal{L}^{(l)}_s(\mathbf{x}_s)$ are already negative, then ξ should be selected as 0 and the Levenberg-Marquardt works as the Netwon method. The proposed algorithm is given under the heading Algorithm 3. The parameter $l_{\max}$ is the maximum number of iterations, and ϵ is a control parameter to determine when to exit the algorithm when the change between two iterations is sufficiently small. We use a controlled increase mechanism for the power control updates. If the difference between the power control parameters during two consecutive time instants is large, this may cause the interference pricing mechanism not to accurately estimate the interference prices [12]. Therefore, we employ the controlled increase mechanism in this paper. The controlled increase mechanism in Step 3 prevents the base stations from changing their transmission powers by a large amount. Therefore, the estimation of the interference levels at the other sectors is accurate. However, the parameter ζ in Algorithm 3 should be selected optimally. Small ζ slows down the algorithm and convergence takes too much time. On the other hand, large ζ fails the purpose of the controlled increase mechanism. Therefore we use an adaptive ζ in this paper. The parameter ζ depends on the current time instant. It is selected as $t/(2t+1)$ [35].

1) Complexity Analysis: The main computational effort of the proposed algorithm is taking the inverse of the matrix $\mathbf{D} = (\nabla^2\mathcal{L}^{(l)}_s - \xi\mathbf{I})$. Therefore, the complexity of the proposed power control increases with the number of power control parameters. When the number of Pico-BSs in the sector increases, the complexity of the algorithm increases with N^3_{Picos}. For example, when there are 2 Pico-BSs in each sector, the matrix becomes 4×4 and taking the inverse of this matrix is straightforward. However, the Pico-BSs are expected to be significantly dense in the future [1]. Taking the inverse of the matrix may not be feasible in real time. Therefore, to overcome this problem, we also propose a suboptimal algorithm. The proposed suboptimal

Algorithm 3: Proposed Power Control Algorithm with Pricing.

Initialize: $\mathbf{z}_s^{(t,0)} = (\varepsilon_M^{(t-1,l_{\max}+1)} \boldsymbol{\beta}_s^{(t-1,l_{\max}+1)^T})$ and set $l = 0$
% Each sector solves (12) by using the Levenberg-Marquardt Method
for $l := 1$ to $l_{\max}$ **do**
  if $\omega_{\max} = \max(\text{ eig}(\nabla^2_{\mathbf{z}} \mathcal{L}_s^{(l)}(\mathbf{x}_s))) < 0$ **then**
    $\xi = 0$.
  else
    $\xi = \omega_{\max} + \sigma$.
  end if
  $\mathbf{d}_l^{LM} = -(\nabla^2 \mathcal{L}_s^{(l)}(\mathbf{x}_s) - \xi \mathbf{I})^{-1} \nabla \mathcal{L}_s^{(l)}(\mathbf{x}_s)$.
  Update the power control parameters, $\mathbf{z}_s^{(l+1)}$, using

$$\mathbf{z}_s^{(t,l+1)} = \mathbf{z}_s^{(t,l)} + \mu_l \mathbf{d}_l^{LM},$$

  Update the Lagrange multiplier, $\lambda_{k,s}^{(l+1)}$ for all $k \in \mathcal{K}_{M,s}^U$, using

$$\lambda_{k,s}^{(l+1)} = \left[\lambda_{k,s}^{(l)} + \phi_{k,s}\left(R_{\min,k} - \left(\boldsymbol{C}_{M,s}^k \boldsymbol{F}_{M,s}^{(k,:)} \boldsymbol{R}_1^{(:,k)} + (1 - \boldsymbol{C}_{M,s}^k) \boldsymbol{F}_{M,s}^{(k,:)} \boldsymbol{R}_2^{(:,k)}\right)\right)\right]^+.$$

  Update the Lagrange multiplier, $\lambda_{k,s}^{(l+1)}$ for all $k \in \mathcal{K}_{P,s}^U$, using

$$\lambda_{k,s}^{(l+1)} = \left[\lambda_{k,s}^{(l)} + \phi_{k,s}\left(R_{\min,k} - \left(\boldsymbol{C}_{M,s}^k \boldsymbol{F}_{M,s}^{(k,:)} \boldsymbol{R}_3^{(:,k)} + (1 - \boldsymbol{C}_{M,s}^k) \boldsymbol{F}_{M,s}^{(k,:)} \boldsymbol{R}_4^{(:,k)}\right)\right)\right]^+.$$

  if $\left|\nabla \mathcal{L}_s^T \mathbf{d}_l^{LM}\right| \leq \epsilon$ **then**
    Break
  end if
end for
$\mathbf{z}_s^{(t,l_{\max}+1)} = (1 - \zeta)\mathbf{z}_s^{(t-1,l_{\max}+1)} + \zeta \mathbf{z}_s^{(t,l_{\max})}$
Price Update: Each user calculates interference prices and feds these values back to its base station.
Interference prices are distributed among base stations.
Go to Step 3 and repeat.

algorithm significantly reduces the complexity of the algorithm and the complexity of the algorithm will be independent of the number of Pico-BSs in the sector.

2) Suboptimal Power Control Algorithm: In the optimal algorithm, all base stations in the sector update their power control parameters together. Therefore, the optimal algorithm reaches the power control parameters that maximize the Lagrangian function. However, this requires calculation of the inverse of matrix $\mathbf{D}$ at every iteration. This becomes computationally costly when the number of Pico-BSs in the sector increases. Therefore, we propose a suboptimal algorithm that calculates the power control parameters of the MBS and Pico-BSs separately. Each base station assumes that the power control parameters of the other base stations in the same sector are constant during updates. The Hessian matrix $\mathbf{D}$ will become 2×2 for MBSs. In addition, Pico-BSs calculate their own power control parameter. Each Pico-BS has only one power control parameter. In simulation results, we will compare the performance of the suboptimal algorithm with the optimal power control algorithm.

V. Numerical Results

In this section, we evaluate the performance of the proposed algorithm. First, we investigate the effect of the parameter α over energy efficiency and spectral efficiency. We show that the proposed algorithm achieves the Pareto optimal solution for all α values. Second, we investigate the effect of the parameter α on outage probabilities. We show that smaller α (i.e., maximizing the energy efficiency of the network) performs better than maximizing spectral efficiency in terms of outage probabilities for this particular setting. Third, we investigate the performance of the proposed frequency assignment algorithm. We evaluate the usage rate of the subbands with different α values and rate constraints. We show that fewer resource blocks are assigned to the users when α and rate constraints increase. Fourth, we investigate the power consumption of the base stations with different α values and minimum rate requirements. We show that MBSs and Pico-BSs show different behavior with increasing rate constraints. While average transmission powers of the MBSs increase with the rate requirements of the users, the average transmission power of the Pico-BSs decreases. Last, we study the performance of the optimum and suboptimal algorithms. We show that the performance of the proposed suboptimal algorithm is close to the optimal algorithm.

First, we will describe our simulation environment. In the FFR method, we distribute the 50 resource blocks with the following approach. First, 14 resource blocks are assigned to subband A, and then the remaining 36 are evenly distributed among the subbandds B, C, and D. In our simulation area, 19 MBSs are deployed and each cell is divided into 3 sectors. Therefore, our simulation area has been divided into 57 sectors. We use the wraparound technique to avoid edge effects. In each sector, two Pico-BSs are randomly deployed. Both MBS and Pico-BSs employ single antennas, i.e., $N_{TRX,M} = 1$ and $N_{TRX,P} = 1$. In each sector, we generate 20 users. First, we generate two users within 40 meters radius of the Pico-BSs. Then, the rest of the users are randomly generated under the settings in Table II. The highest RSRP method is used for the cell associations. Even though we generate two users close to Pico-BSs, they are not forced to associate with the Pico-BSs. The rest of the simulation parameters are given in Table II [36].

Fig. 3 illustrates the average energy efficiency and the spectral efficiency of the sectors for different α values for five cases. In the first case, users do not have any rate constraints. For the other cases, the following rate constraints are enforced: 8 kbps, 32 kbps, 128 kbps, and 512 kbps. As expected, the average energy efficiency of the network decreases with α for all cases. When users do not have minimum rate constraint and α is equal to 0, the average energy efficiency of the network reaches its

TABLE II
SIMULATION PARAMETERS

Parameter	Setting
Channel bandwidth	10 MHz
Total number of RBs	50 RBs
Freq. selective channel model (CM)	Extended Typical Urban CM
UE to MBS PL model	$128.1 + 37.6 \log_{10}(d)$
UE to Pico eNB PL model	$140.7 + 36.7 \log_{10}(d)$
Effective thermal noise power, N_0	-174 dBm/ Hz
UE noise figures	9 dB
MBS and Pico eNB antenna gain	14 dBi and 5 dBi
UE antenna gain	0 dBi
Antenna horizontal pattern, $A(\theta)$	$-\min(12(\theta/\theta_{3\text{dB}})^2, A_m)$
A_m and $\theta_{3\text{dB}}$	20 dB and 70°
Penetration loss	20 dB
Macrocell and picocell shadowing	8 dB and 10 dB
Inter-site distance	500 m
Minimum MBS to user distance	50 m
Minimum Pico-BS to user distance	10 m
Minimum Pico-BS to MBS distance	75 m
Minimum Pico-BS to Pico-BS distance	40 m
Traffic model	Full buffer
Power Consumption Parameters	MBS: (130 W, 75 W, 46 dBm, 4.7)
$(P_0, P_{sleep}, P_{\max}, \Delta)$	Pico-eNB: (56 W, 39 W, 30 dBm, 2.6)

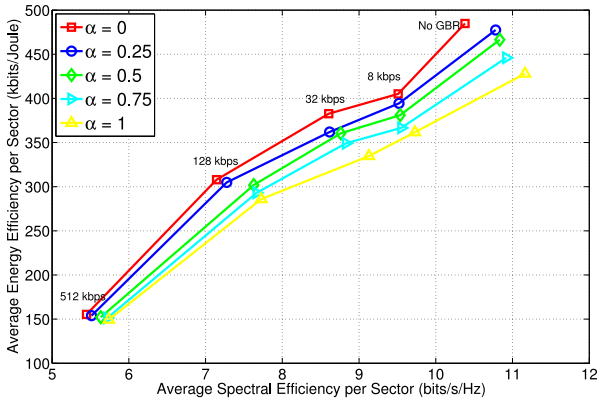

Fig. 3. The average energy efficiency versus average spectral efficiency per sector for different α values.

highest point and it becomes 484.83 kbits/Joule. When we increase α for this case, the energy efficiency of the network decreases with α as expected. When α becomes 1 (i.e., the objective becomes maximizing the spectral efficiency of the network), the average energy efficiency drops by 13%. When the parameter α increases, the transmission power of the MBSs increases with α in order to increase the spectral efficiency. For example, the average transmission power of the MBSs increases from 23.94 dBm to 29.68 dBm when α increases from 0 to 1. Although this change increases the spectral efficiency of the network by 7%, it also causes the MBSs to work in the energy-inefficient regions. In other words, by increasing α from 0 to 1, 13% energy efficiency sacrifice can be turned into 7% gain in terms of spectral efficiency when users do not have any rate requirements. On the other hand, the average transmission power of Pico-BSs is not affected by α when users do not have minimum rate constraints and they always transmit at the full power. Due to the fact that the power consumptions of Pico-BSs are less than those of the MBSs and the distance between Pico-BSs and the associated users is low, both energy efficiency and spectral efficiency of the Pico-BSs increase with parameter β within the given ranges. In other words, the most energy-efficient state and the most spectrally-efficient state coincide for these base stations. When users have minimum rate constraints, both energy efficiency and spectral efficiency of the network decrease. The cumulative effect of the following reasons cause this drop. First, in order to satisfy the rate requirements of users, MBSs further increase their transmission powers to energy-inefficient levels. This increase elevates the cross-tier interference from MBS to cell-edge Pico-BSs on Subband A and also intercell interference in the network. Second, the frequency assignment algorithm favors users that cannot satisfy their rate requirement. These users usually have worse channel conditions than the other users. Therefore, both energy efficiency and spectral efficiency are harmed by the change in frequency assignment. As a result of all these factors, both energy efficiency and the spectral efficiency of the network decrease with the minimum rate requirements of the users.

TABLE III
THE OUTAGE PROBABILITIES OF USERS FOR DIFFERENT α VALUES

	Outage probability			
Minimum	$\alpha = 0$		$\alpha = 1$	
GBR (kbps)	MUE	PUE	MUE	PUE
8	0.8%	0%	1.1%	0%
32	1.7%	0%	2.4%	0%
128	3.1%	0.6%	4.3%	0.6%
512	9.6%	2%	12.3%	0.6%

In addition, when we increase the minimum rate requirements of the users, the effect of the parameter α on energy efficiency and spectral efficiency decreases. For example, as specified earlier, 7% spectral efficiency loss can be turned into 13% energy efficiency gain when users do not have any rate requirements. On the other hand, when the minimum rate requirements of users are 512 kbps, 5% spectral efficiency loss can only be turned into 4% energy efficiency gain. These results show that when users have minimum rate requirements, the proposed algorithm prioritizes satisfying the rate requirements of more users and the effect of parameter α on energy efficiency and spectral efficiency decreases. Note from Fig. 3 that for the no-rate-constraint-case, improving energy efficiency decreases spectral efficiency and vice versa. Therefore, all points on this curve $(\eta_s(\boldsymbol{\varepsilon}, \boldsymbol{\beta}), \nu_s(\boldsymbol{\varepsilon}, \boldsymbol{\beta}))$ are Pareto optimal for $0 \leq \alpha \leq 1$.

Second, we investigate the relation between the parameter α and outage probabilities. In Table III, we investigate four cases, the minimum rate requirements of users are 8 kbps, 32 kbps, 128 kbps, and 512 kbps. The outage probability is not defined when users do not have a minimum rate requirement. In our network, we have two different type of users: MUEs and PUEs. First, we observe that when we increase the parameter α, the outage probabilities of the MUEs increase with α for all four cases. For example, when the minimum rate requirement of the

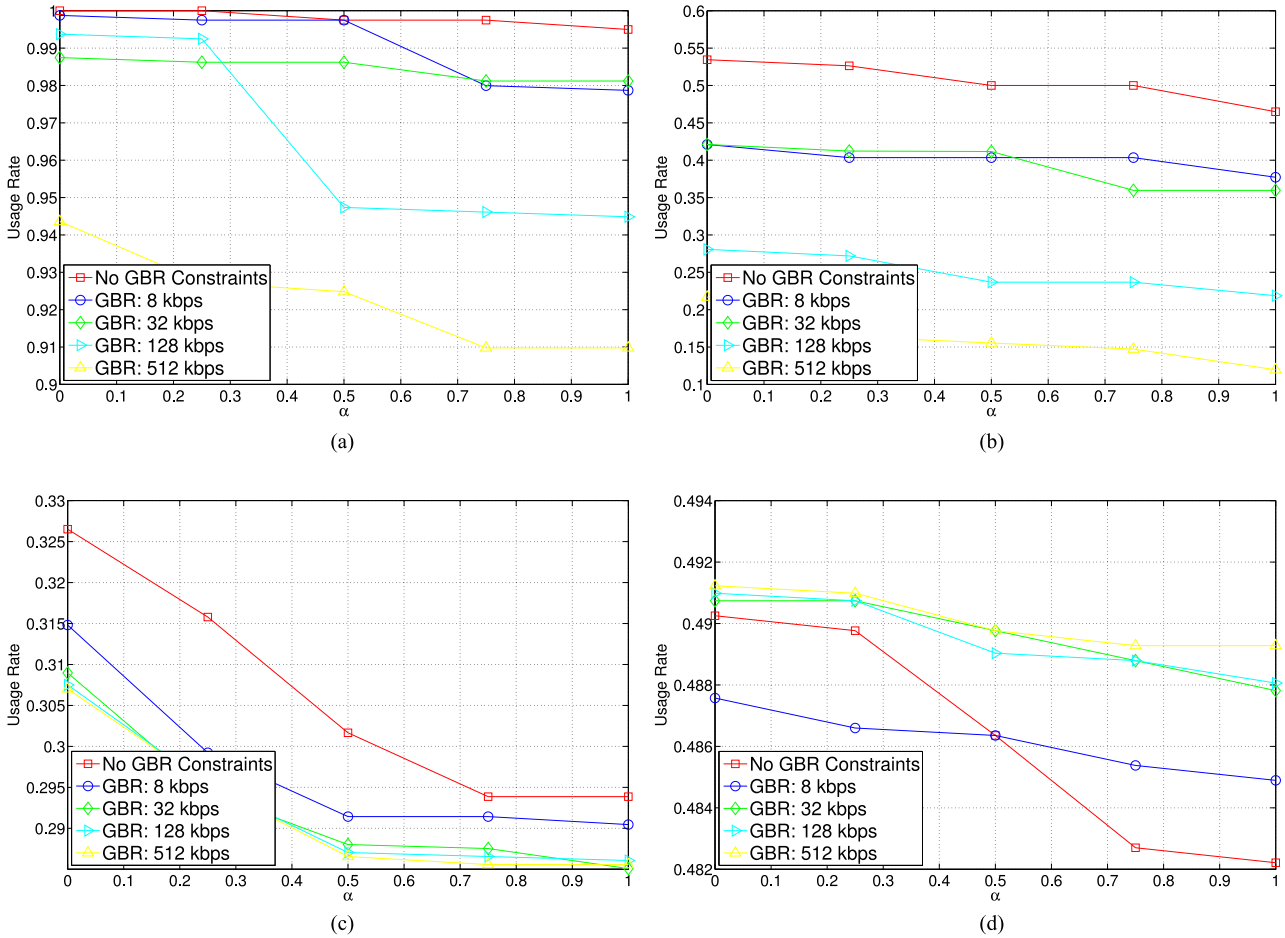

Fig. 4. (a) Average usage rate of subband A by MBSs, (b) average usage rate of subband A by pico-BSs, (c) average usage rate of subbands B, C, and D by MBSs, and (d) average usage rate of subbands B, C, and D by pico-BSs for different α values.

users is 512 kbps, changing α from 0 to 1 increases the outage probability of MUEs from 9.6% to 12.3%. Similar behavior can also be observed for the other cases. When the parameter α increases, the transmission powers of MBSs and Pico-BSs increase with this parameter. For example, when we change the parameter α from 0 to 1, the transmission powers of the Pico-BSs increase from 27.7 dBm to 28.4 dBm for the case that minimum rate requirements of the users are 512 kbps. Although this change increases the average spectral efficiency of the network, cross-tier interference from Pico-BSs to MUEs increases the outage probability of MUEs. In the same manner, the transmission power increase of MBSs elevates the intercell interference and that is another reason of the increased outage probabilities. On the other hand, the outage probabilities of the PUEs only exists when the minimum rate requirements of users are high. However, even for the worst case, only 2% of the PUEs could not satisfy their rate requirements. In the network, PUEs are located close to their associated Pico-BSs and they have significantly better channel conditions than the MUEs. In addition, the number of PUEs that are associated with each Pico-BS is significantly lower. Therefore, more resource blocks are assigned to these users on average. As a result, PUEs can satisfy their rate requirements easier than MUEs.

Fig. 4(a)–(d) show the average usage rate of the subbands A by MBSs, subbands A by Pico-BSs, subbands B, C, and D by MBSs, and subbands B, C, and D by Pico-BSs, respectively. First, we observe that when we increase the minimum rate requirements of the users, the usage of the resource blocks by MBSs decreases. The second part of the proposed frequency assignment algorithm decreases the number of assigned resource blocks and transmits on the fewer resource blocks. For example, MBSs use almost all assigned resource blocks for all different α values when users do not have minimum rate requirements. However, when users have minimum rate requirements, MBSs decide not to assign some of the available resource blocks. When the minimum rate requirements of the users increase, intercell interference becomes a more significant problem, due to the fact that base stations increase their transmission power to satisfy the rate requirements of their users. In order to alleviate the interference, base stations do not assign the resource blocks that do not increase the energy efficiency and spectral efficiency while creating significant interference to other base stations. Fig. 4(b) illustrates that usage rate of subband A by Pico-BSs significantly decreases when we increase the minimum rate of the users. The reason for this decrease is twofold. First, cell-edge Pico-BSs do not assign some resource blocks on subband A to help

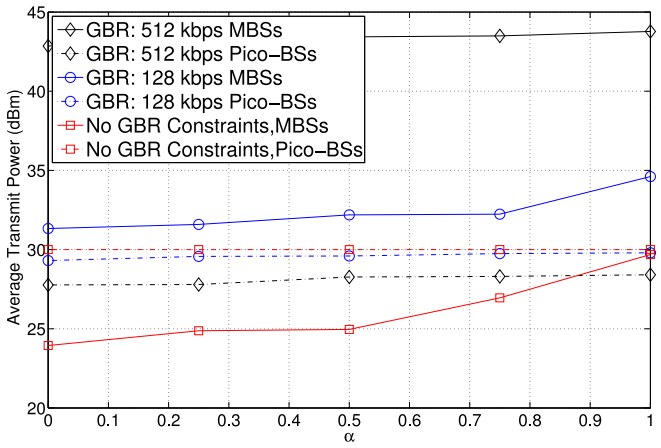

Fig. 5. The average transmission power of MBSs and Pico-BSs for different α values for different rate requirements.

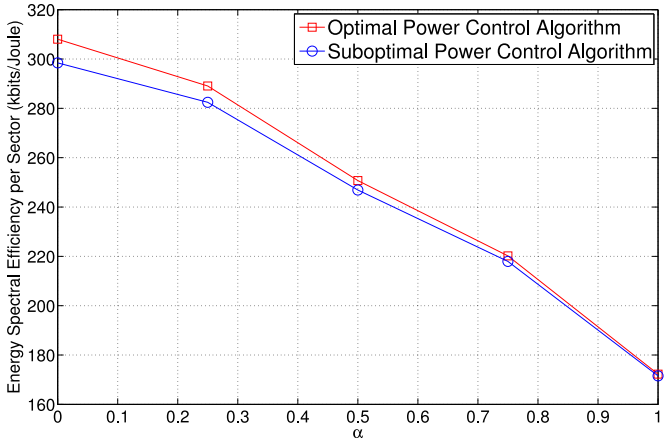

Fig. 6. The average energy spectral efficiency of network for different α values when minimum rate constraints are 128 kbps.

satisfy the minimum rate constraints of the cell-center MUEs in the same sector. Second, cell-center radii expand with the minimum rate requirements. Therefore, the number of Pico-BSs that are located in the cell-edge region decreases and fewer Pico-BSs will use subband A. Another important observation is when we increase the parameter α, the usage of the resource blocks further decreases. In order to increase the spectral efficiency of the network, base stations decide to transmit on the resource blocks that have better channel quality and do not assign the others to increase the overall spectral efficiency of the network. Therefore, when we increase α, the subband usage further decreases to improve the spectral efficiency of the network.

Fig. 5 shows the average power consumption of the MBSs and Pico-BSs for the following cases: No rate requirement and rate requirements equal to 128 kbps and 512 kbps. Similar observations can be made for the other rate requirements. As expected, when we increase the minimum rate requirements, the transmission power of the MBSs increases. On the other hand, under the same conditions, the transmission power of the Pico-BSs decreases. The increase of the minimum rate constraints causes outage of the more MUEs. In order to satisfy these users' rate requirements, MBSs increase their transmission power, increase the interference prices, and assign more resource blocks to these users. Elevated interference prices force some of the Pico-BSs to decrease their transmission power to help satisfy the rate requirements of more MUEs. Therefore, the average transmission power of the Pico-BSs decreases with the minimum rate requirements. In addition, the average transmission power of both MBSs and Pico-BSs increases with parameter α to increase the spectral efficiency of the network.

Fig. 6 compares the performance of the suboptimal and optimal power control algorithms in terms of energy efficiency and spectral efficiency when the minimum rate requirements of users are 128 kbps. The performance of both algorithms is similar. When $\alpha = 0$, the optimal algorithm performs 3.2% better than the suboptimal algorithm. On the other hand, when $\alpha = 1$, the performance difference drops to 0.4%. In the suboptimal power control algorithm, MBS and Pico-BSs update their power control parameters separately. The transmission powers of the base stations increase with the parameter α, therefore the difference between the performance of these algorithms decreases.

VI. Conclusion

In this paper, we studied the energy efficiency and spectral efficiency tradeoffs in multi-cell heterogeneous wireless networks. We defined the problem as multi-objective optimization and proposed a cell-center radius selection algorithm, a scheduling algorithm, and a power control algorithm that solve these problems separately. The proposed algorithm also includes the minimum rate requirements of users to the given problem. A dynamic cell-center radius selection algorithm is proposed to determine the available resources to the base stations. In addition, the proposed scheduling mechanism has distributed the resources to users in order to satisfy the minimum rate requirements of them and also to maximize our objective metric. Furthermore, we employed a Levenberg-Marquardt method-based power allocation algorithm to solve the power control problem. Based on our results, first the tradeoff between energy efficiency and spectral efficiency can be adjusted via the weight of the multi-objective function. We can obtain 13% improvement in terms of energy efficiency by sacrificing 7% spectral efficiency. In addition, our results show that the most energy-efficient state and the most spectral efficient state coincide for the Pico-BSs. Second, while we increase the spectral efficiency of the network, it also increases the outage probabilities of the network due to the increased intercell-interference. Third, we showed that the number of resource blocks that are transmitted can be reduced by increasing the minimum rate constraints or the parameter α. Fourth, we demonstrated that while the transmission powers of the MBSs increase with the minimum rate constraints of the users, the transmission power of Pico-BSs decreases. Last, we studied the optimal and a suboptimal power control algorithms. We showed that these algorithms perform similarly and increasing the parameter α, shrinks the gap between these algorithms.

REFERENCES

[1] Qualcomm, "Rising to meet the 1000x mobile data challenge," White Paper, Jun. 2012.

[2] K. Davaslioglu and E. Ayanoglu, "Quantifying potential energy efficiency gain in green cellular wireless networks," *IEEE Commun. Surveys Tuts.*, vol. 16, no. 4, pp. 2065–2091, Fourth Quarter 2014.

[3] A. Ghosh *et al.*, "Heterogeneous cellular networks: From theory to practice," *IEEE Commun. Mag.*, vol. 50, no. 6, pp. 54–64, Jun. 2012.

[4] S. Yunas, M. Valkama, and J. Niemelä, "Spectral and energy efficiency of ultra-dense networks under different deployment strategies," *IEEE Commun. Magaz.*, vol. 53, no. 1, pp. 90–100, Jan. 2015.

[5] G. Boudreau, J. Panicker, N. Guo, R. Chang, N. Wang, and S. Vrzic, "Interference coordination and cancellation for 4G networks," *IEEE Commun. Mag.*, vol. 47, no. 4, pp. 74–81, Apr. 2009.

[6] H. Holma and A. Toskala, *LTE-Advanced: 3GPP Solution for IMT-Advanced*. West Sussex, U.K.: Wiley, 2012.

[7] N. Saquib, E. Hossain, and D. I. Kim, "Fractional frequency reuse for interference management in LTE-Advanced HetNets," *IEEE Wireless Commun.*, vol. 20, no. 2, pp. 113–122, Apr. 2013.

[8] K. Davaslioglu, C. Coskun, and E. Ayanoglu, "Energy-efficient resource allocation for fractional frequency reuse in heterogeneous networks," *IEEE Trans. Wireless Commun.*, vol. 14, no. 10, pp. 5484–5497, Oct. 2015.

[9] C. C. Coskun, K. Davaslioglu, and E. Ayanoglu, "Three-stage resource allocation algorithm for energy-efficient heterogeneous networks," *IEEE Trans. Veh. Technol.*, vol. 66, no. 8, pp. 6942–6957, Aug. 2017.

[10] C. Saraydar, N. B. Mandayam, and D. Goodman, "Pricing and power control in a multicell wireless data network," *IEEE J. Sel. Areas Commun.*, vol. 19, no. 10, pp. 1883–1892, Oct. 2001.

[11] J. Huang, R. Berry, and M. Honig, "Distributed interference compensation for wireless networks," *IEEE J. Sel. Areas Commun.*, vol. 24, no. 5, pp. 1074–1084, May 2006.

[12] C. Shi, R. Berry, and M. Honig, "Distributed interference pricing for OFDM wireless networks with non-separable utilities," in *Proc. Annu. Conf. Inf. Sci. Syst.*, Mar. 2008, pp. 755–760.

[13] C. Shi, R. Berry, and M. Honig, "Monotonic convergence of distributed interference pricing in wireless networks," in *Proc. IEEE Int. Symp. Inf. Theory*, Jun. 2009, pp. 1619–1623.

[14] C. Xiong, G. Li, S. Zhang, Y. Chen, and S. Xu, "Energy- and spectral-efficiency tradeoff in downlink OFDMA networks," *IEEE Trans. Wireless Commun.*, vol. 10, no. 11, pp. 3874–3886, Nov. 2011.

[15] D. Tsilimantos, J. Gorce, and K. Jaffr ès-Runser, "Spectral and energy efficiency trade-off with joint power-bandwidth allocation in OFDMA networks," *CoRR*, vol. abs/1311.7302, 2013.

[16] Y. Li, M. Sheng, C. Yang, and X. Wang, "Energy efficiency and spectral efficiency tradeoff in interference-limited wireless networks," *IEEE Commun. Lett.*, vol. 17, no. 10, pp. 1924–1927, Oct. 2013.

[17] R. Marler and J. Arora, "Survey of multi-objective optimization methods for engineering," *Struct. Multidiscip. Optim.*, vol. 26, no. 6, pp. 369–395, 2004.

[18] L. Deng, Y. Rui, P. Cheng, J. Zhang, Q. Zhang, and M. Li, "A unified energy efficiency and spectral efficiency tradeoff metric in wireless networks," *IEEE Commun. Lett.*, vol. 17, no. 1, pp. 55–58, Jan. 2013.

[19] J. Rao and A. Fapojuwo, "On the tradeoff between spectral efficiency and energy efficiency of homogeneous cellular networks with outage constraint," *IEEE Trans. Veh. Technol.*, vol. 62, no. 4, pp. 1801–1814, May 2013.

[20] W. Jing, Z. Lu, X. Wen, Z. Hu, and S. Yang, "Flexible resource allocation for joint optimization of energy and spectral efficiency in OFDMA multi-cell networks," *IEEE Commun. Lett.*, vol. 19, no. 3, pp. 451–454, Mar. 2015.

[21] C. He, B. Sheng, P. Zhu, X. You, and G. Li, "Energy- and spectral-efficiency tradeoff for distributed antenna systems with proportional fairness," *IEEE J. Sel. Areas Commun.*, vol. 31, no. 5, pp. 894–902, May 2013.

[22] J. Tang, D. So, E. Alsusa, and K. Hamdi, "Resource efficiency: A new paradigm on energy efficiency and spectral efficiency tradeoff," *IEEE Trans. Wireless Commun.*, vol. 13, no. 8, pp. 4656–4669, Aug. 2014.

[23] C. Yang, J. Li, A. Anpalagan, and M. Guizani, "Joint power coordination for spectral-and-energy efficiency in heterogeneous small cell networks: A bargaining game-theoretic perspective," *IEEE Trans. Wireless Commun.*, vol. 15, no. 2, pp. 1364–1376, Feb. 2016.

[24] C. C. Coskun and E. Ayanoglu, "Energy-spectral efficiency tradeoff for heterogeneous networks with QoS constraints," in *Proc. IEEE Int. Conf. Commun.*, May 2017, pp. 1–7.

[25] G. Auer *et al.*, "How much energy is needed to run a wireless network?" *IEEE Wireless Commun.*, vol. 18, no. 5, pp. 40–49, Oct. 2011.

[26] F. Richter, A. Fehske, and G. Fettweis, "Energy efficiency aspects of base station deployment strategies for cellular networks," in *Proc. IEEE Veh. Technol. Conf.*, Sep. 2009, pp. 1–5.

[27] H. Holtkamp, G. Auer, V. Giannini, and H. Haas, "A parameterized base station power model," *IEEE Commun. Lett.*, vol. 17, no. 11, pp. 2033–2035, Nov. 2013.

[28] L. Hoo, B. Halder, J. Tellado, and J. Cioffi, "Multiuser transmit optimization for multicarrier broadcast channels: Asymptotic FDMA capacity region and algorithms," *IEEE Trans. Commun.*, vol. 52, no. 6, pp. 922–930, Jun. 2004.

[29] W. Yu, "Multiuser water-filling in the presence of crosstalk," in *Proc. Inf. Theory Appl. Workshop*, Jan. 2007, pp. 414–420.

[30] S. Sesia, I. Toufik, and M. Baker, *LTE—The UMTS Long Term Evolution: From Theory to Practice*. West Sussex, U.K.: Wiley, 2009.

[31] C. C. Coskun and E. Ayanoglu, "Energy-spectral efficiency trade-off for heterogeneous networks with QoS constraints (Appendix)," Oct. 2016. [Online]. Available: http://newport.eecs.uci.edu/ ayanoglu/EESE.pdf

[32] C. Saraydar, N. B. Mandayam, and D. Goodman, "Efficient power control via pricing in wireless data networks," *IEEE Trans. Commun.*, vol. 50, no. 2, pp. 291–303, Feb. 2002.

[33] M. S. Bazaraa, H. D. Sherali, and C. M. Shetty, *Nonlinear Programming: Theory and Algorithms*. New York, NY, USA: Wiley, 1993.

[34] P. M. Pardalos and M. G. C. Resende, Eds., *Handbook of Applied Optimization*. New York, NY, USA: Oxford Univ. Press, 2002.

[35] Z. Han, D. Niyato, W. Saad, T. Başar, and A. Hjørungnes, *Game Theory in Wireless and Communication Networks: Theory, Models, and Applications*. Cambridge, U.K.: Cambridge Univ. Press, 2012.

[36] *Further Advancements for E-UTRA Physical Layer Aspects (Release 9)*, 3GPP, TR 36.814, Mar. 2010.

Cemil Can Coskun (S'07–M'17) received the bachelor's and master's degrees in electrical and electronics engineering from Bilkent University, Ankara, Turkey, in 2010 and 2012, respectively, and the Ph.D. degree in electrical and computer engineering, University of California, Irvine, CA, USA, in 2017, where he was affiliated with the Center for Pervasive Communications and Computing. His research interests include the area on resource allocation in wireless networks, small-cell base station deployment in wireless networks, green communications, and energy efficiency and spectral efficiency tradeoff in wireless networks.

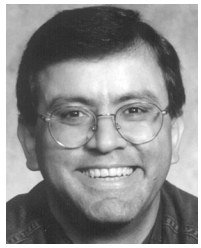

Ender Ayanoglu (S'82–M'85–SM'90–F'98) received the Ph.D. degree in electrical engineering from Stanford University, Stanford, CA, USA, in 1986. He was with the Communications Systems Research Laboratory, Holmdel, NJ, USA, part of AT&T Bell Laboratories, until 1996, and Bell Laboratories, Lucent Technologies, from 1996 to 1999. From 1999 to 2002, he was a Systems Architect with Cisco Systems, Inc., San Jose, CA. Since 2002, he has been a Professor with the Department of Electrical Engineering and Computer Science, University of California, Irvine, CA, where he served as the Director of the Center for Pervasive Communications and Computing and the Conexant-Broadcom Endowed Chair from 2002 to 2010. His past accomplishments include invention of 56K modems, characterization of wavelength conversion gain in wavelength-division multiplexed systems, and diversity coding. From 2000 to 2001, he served as the Founding Chair of the IEEE-ISTO Broadband Wireless Internet Forum, an industry standards organization. He served on the Executive Committee of the IEEE Communications Society's Communication Theory Committee from 1990 to 2002 and the Chair from 1999 to 2002. From 1993 to 2014, he was an Editor of the IEEE TRANSACTIONS ON COMMUNICATIONS. He served as the Editor-in-Chief of the IEEE TRANSACTIONS ON COMMUNICATIONS from 2004 to 2008 and the IEEE JOURNAL ON SELECTED AREAS IN COMMUNICATIONS series on Green Communications and Networking from 2014 to 2016. Since 2014, he has been a Senior Editor of the IEEE TRANSACTIONS ON COMMUNICATIONS. Since 2016, he has been serving as the Founding Editor-in-Chief of the IEEE TRANSACTIONS ON GREEN COMMUNICATIONS AND NETWORKING. He received the IEEE Communications Society Stephen O. Rice Prize Paper Award in 1995, the IEEE Communications Society Best Tutorial Paper Award in 1997, and the IEEE Communications Society Communication Theory Technical Committee Outstanding Service Award in 2014.